AD-A234 602

OFFICE OF NAVAL RESEARCH

Contract N00014-84-G-0201

Task No. 0051-865

Technical Report #38

The Control of Orbital Mixing in Ruthenium Complexes Containing Quinone Related Ligands

By

H. Masui, A.B.P. Lever*, and P.R. Auburn

in

Inorganic Chemistry

York University
Department of Chemistry, 4700 Keele St., North York
Ontario, Canada M3J 1P3

Reproduction in whole, or in part, is permitted for any purpose of the United States Government

*This document has been approved for public release and sale; its distribution is unlimited

*This statement should also appear in item 10 of the Document Control Data DD form 1473. Copies of the form available from cognizant contract administrator

91 4 18 002

SECURITY CLASSIFICATION OF THIS PAGE

REPORT DOCUMENTATION PAGE

1a. REPORT SECURITY CLASSIFICATION	1b RESTRICTIVE MARKINGS
2a. SECURITY CLASSIFICATION AUTHORITY Unclassified	3 DISTRIBUTION / AVAILABILITY OF REPORT As it appears on the report
2b DECLASSIFICATION / DOWNGRADING SCHEDULE	
4 PERFORMING ORGANIZATION REPORT NUMBER(S) Report # 38	5. MONITORING ORGANIZATION REPORT NUMBER(S)
6a. NAME OF PERFORMING ORGANIZATION A.B.P. Lever, York University Chemistry Department 6b OFFICE SYMBOL (If applicable)	7a NAME OF MONITORING ORGANIZATION Office of Naval Research
6c. ADDRESS (City, State, and ZIP Code) 4700 Keele St., North York, Ontario M3J 1P3 Canada	7b ADDRESS (City, State, and ZIP Code) Chemistry Division 800 N. Quincy Street Arlington, VA 22217 U.S.A.
8a. NAME OF FUNDING / SPONSORING ORGANIZATION 8b OFFICE SYMBOL (If applicable)	9 PROCUREMENT INSTRUMENT IDENTIFICATION NUMBER N00014-84-G-0201
8c. ADDRESS (City, State, and ZIP Code)	10 SOURCE OF FUNDING NUMBERS PROGRAM ELEMENT NO. / PROJECT NO. / TASK NO / WORK UNIT ACCESSION NO

11 TITLE (Include Security Classification)
The Control of Orbital Mixing in Ruthenium Complexes Containing Quinone Related Ligands

12 PERSONAL AUTHOR(S)
H. Masui, A.B.P. Lever* and P.R. Auburn

13a. TYPE OF REPORT	13b. TIME COVERED	14 DATE OF REPORT (Year, Month, Day)	15 PAGE COUNT
Technical	FROM Aug.'90 TO Aug.'91	April 4, 1991	38

16. SUPPLEMENTARY NOTATION

17 COSATI CODES			18 SUBJECT TERMS (Continue on reverse if necessary and identify by block number)
FIELD	GROUP	SUB-GROUP	Quinone, Ruthenium, Electronic Structure, Orbital Mixing, Electrochemistry, Optical Spectroscopy

19 ABSTRACT (Continue on reverse if necessary and identify by block number)

Three redox series of complexes of the general formula Ru(II)(bpy)$_2$LL and Ru(II)(Py)$_4$LL (bpy=2,2'-bipyridine) are reported, where LL are the ligands, 1,2-dihydroxybenzene, 2-aminophenol or 1,2-diaminobenzene. These ligands can exist in the fully reduced catechol form, or the one and two electron oxidized semiquinone and quinone forms. Electronic and electron spin resonance spectroscopic, and electrochemical data are discussed in terms of orbital mixing and electronic structure, and the number of oxygen or nitrogen atoms in the coordinating ligand.

20 DISTRIBUTION / AVAILABILITY OF ABSTRACT	21 ABSTRACT SECURITY CLASSIFICATION
☒ UNCLASSIFIED/UNLIMITED ☐ SAME AS RPT ☐ DTIC USERS	Unclassified/unlimited
22a NAME OF RESPONSIBLE INDIVIDUAL Dr. Ronald A. De Marco	22b TELEPHONE (Include Area Code) / 22c OFFICE SYMBOL

DD FORM 1473, 84 MAR 83 APR edition may be used until exhausted
All other editions are obsolete

SECURITY CLASSIFICATION OF THIS PAGE

1990

TECHNICAL REPORT DISTRIBUTION LIST - GENERAL

Office of Naval Research (2)
Chemistry Division, Code 1113
800 North Quincy Street
Arlington, Virginia 22217-5000

Dr. Robert Green, Director (1)
Chemistry Division, Code 385
Naval Weapons Center
China Lake, CA 93555-6001

Commanding Officer (1)
Naval Weapons Support Center
Dr. Bernard E. Douda
Crane, Indiana 47522-5050

Chief of Naval Research (1)
Special Assistant for Marine
Corps Matters
Code 00MC
800 North Quincy Street
Arlington, VA 22217-5000

Dr. Richard W. Drisko (1)
Naval Civil Engineering
Laboratory
Code L52
Port Hueneme, CA 93043

Dr. Bernadette Eichinger (1)
Naval Ship Systems Engineering
Station
Code 053
Philadelphia Naval Base
Philadelphia, PA 19112

David Taylor Research Center (1)
Dr. Eugene C. Fischer
Annapolis, MD 21402-5067

Dr. Sachio Yamamoto (1)
Naval Ocean Systems Center
Code 52
San Diego, CA 92152-5000

Dr. James S. Murday (1)
Chemistry Division, Code 6100
Naval Research Laboratory
Washington, D.C. 20375-5000

Dr. Harold H. Singerman (1)
David Taylor Research Center
Code 283
Annapolis, MD 21402-5067

Defense Technical Information Center (2)
Building 5, Cameron Station
Alexandria, VA 22314

✓

A-1

ENCLOSURE(2)

ONR Electrochemical Sciences Program
Robert J. Nowak, Program Manager

Professor Hector Abruña
Department of Chemistry
Cornell University
Ithaca, NY 14853
413d018

Professor C. A. Angell
Arizona State University
Department of Chemistry
Tempe, AZ 85287
413d007

Professor Allen Bard
Department of Chemistry
The University of Texas at Austin
Austin, TX 78712-1167
413a002

Professor Lesser Blum
Department of Physics
University of Puerto Rico
Rio Piedras, PUERTO RICO 00931
4133002

Professor James Brophy
Department of Physics
University of Utah
Salt Lake City, UT 84112
413d015

Professor Daniel Buttry
Department of Chemistry
University of Wyoming
Laramie, WY 82071
4133019

Professor Bruce Dunn
Departement of Materials Science and Engineering
University of California, Los Angeles
Los Angeles, CA 90024
413d011

Professor Andrew Ewing
Department of Chemistry
152 Davey Laboratory
Pennsylvania State University
University Park, PA 16802
4133030

Professor Gregory Farrington
Laboratory for Research on the Structure of Matter
3231 Walnut Street
Philadelphia, PA 19104-6202
413d003

Professor W. R. Fawcett
Department of Chemistry
University of California, Davis
Davis, CA 95616
4133020

Professor Martha Greenblatt
Department of Chemistry
Rutgers University
Piscataway, NJ 08854
413d008

Professor Joel Harris
Department of Chemistry
University of Utah
Salt Lake City, UT 84112
413a005

Professor Adam Heller
Department of Chemical Engineering
University of Texas at Austin
Austin, TX 78712-1062
413h007

Professor Pat Hendra
The University
Southampton SO9 5NH
ENGLAND
4134001

ONR Electrochemical Sciences Program
Robert J. Nowak, Program Manager

Professor Joseph Hupp
Department of Chemistry
Northwestern University
Evanston, IL 60208
4133025

Professor D. E. Irish
Department of Chemistry
University of Waterloo
Waterloo, Ontario, CANADA N21 3G1
4133017

Professor A. B. P. Lever
Department of Chemistry
York University
4700 Keele Street
North York, Ontario M3J 1P3
4131025

Professor Nathan S. Lewis
Division of Chemistry and Chemical Engineering
California Institute of Technology
Pasadena, CA 91125
413d017

Professor Rudolph Marcus
Division of Chemistry and Chemical Engineering
California Institute of Technology
Pasadena, CA 91125
4133004

Professor Charles Martin
Department of Chemistry
Texas A&M University
College Station, TX 77843
413d005

Professor Royce W. Murray
Department of Chemistry
University of North Carolina
Chapel Hill, NC 27514
4133015

Dr. Michael R. Philpott
IBM Research Division
Almaden Research Center
650 Harry Road
San Jose, CA 95120-6099
4133011

Professor Richard Pollard
Department of Chemical Engineering
University of Houston, University Park
4800 Calhoun, Houston, TX 77004
413d016

Professor B. S. Pons
Department of Chemistry
University of Utah
Salt Lake City, UT 84112
4133010

Dr. Donald Sandstrom
Boeing Aerospace Company
P.O. Box 3999, M/S 87-08
Seattle, WA 98124-2499
4133007

Professor Jack Simons
Department of Chemistry
University of Utah
Salt Lake City, UT 84112
4131050

ONR Electrochemical Sciences Program
Robert J. Nowak, Program Manager

Dr. H. Gilbert Smith
EG&G Mason Research Institute
57 Union Street
Worcester, MA 01608
413k003

Dr. Stanislaw Szpak
Code 634
Naval Ocean Systems Center
San Diego, CA 92152-5000
4131006

Professor Michael Weaver
Department of Chemistry
Purdue University
West Lafayette, IN 49707
4133001

Professor Geroge Wilson
Department of Chemistry
University of Kansas
Lawrence, KS 66045
413k002

Professor Ernest Yeager
Case Center for Electrochemical
Sciences
Case Western Reserve University
Cleveland, OH 44106
4133008

Professor Ulrich Stimming
Department of Chemical Engineering
and Applied Chemistry
Columbia University
New York, NY 10027
4133014

Professor Petr Vanýsek
Department of Chemistry
Northern Illinois University
Dekalb, IL 60115
413k001

Professor Henry White
Department of Chemical Engineering
and Materials Science
421 Washington Ave., SE
Minneapolis, MN 55455
400o027yip

Professor Mark S. Wrighton
Department of Chemistry
Massachusetts Institute of Techno...
Cambridge, MA 02139
4131027

INORG. CHEM.
2 MAY 1991

Contribution from the Dept. of Chemistry, York University,
North York (Toronto),
Ontario, Canada, M3J 1P3.

The Control of Orbital Mixing in Ruthenium Complexes Containing Quinone Related Ligands

By Hitoshi Masui, A. B. P. Lever*, and Pamela R. Auburn.

Abstract.

Three redox series of complexes of the general formula $Ru(II)(bpy)_2LL$ and $Ru(II)(Py)_4LL$ (bpy = 2,2'-bipyridine) are reported, where LL are the ligands, 1,2-dihydroxybenzene, 2-aminophenol or 1,2-diaminobenzene. These ligands can exist in the fully reduced catechol form, or the one and two electron oxidized semiquinone and quinone forms. Electronic and electron spin resonance spectroscopic, and electrochemical data are discussed in terms of orbital mixing and electronic structure, and the number of oxygen or nitrogen atoms in the coordinating ligand.

Introduction

There has been considerable interest in the study of transition metal complexes of non-innocent, quinone-related ligands including those of dithiolenes,[1-3] dioxolenes,[4-16] and benzoquinonediimines.[17-33] The possibility of electron delocalization between the metal and the ligand has been a major theme in the study of these systems.[30,34-36] The electron distribution will depend on the extent of mixing between the metal and ligand orbitals which, in turn, is a function of the energies, symmetries and overlap of the valence metal and ligand orbitals.

Previous studies of ruthenium dioxolene complexes (dioxolene = catechol, semiquinone, and quinone)[7-9] have found unusually large degrees of orbital mixing between the metal and the ligand. The successive substitution of the dioxolene oxygen atoms with less electronegative nitrogen atoms may be expected to change this mixing in a systematic fashion depending upon ligand charge and oxidation state.

To investigate the effects of such variations, a series of ruthenium complexes were synthesized containing orthophenylene ligands (Scheme 1). The orthophenylene ligands, which include catechols, (oo), o-aminophenols, (no), and orthophenylenediamines, (nn), have three easily accessed redox forms:-the fully reduced catechol form, $catH_n$, the partially oxidized semiquinone form, sqH_n, and the fully oxidized quinone form, qH_n which can exist in various states of protonation. The subscript, n, reflects the number of protons attached to the donor atoms in each species. Scheme 1

The synthesis of three compounds by successive replacement of the oxygen atoms by nitrogen yields, through permutation of the three oxidation states, nine species whose orbital energies can be probed via their rich electronic spectra. These orthophenylene ligands form fairly stable semiquinone complexes whose electron spin resonance (ESR) spectra may also be used to estimate the degree of orbital mixing within the complexes.

Reported here are the synthesis and characterization by electrochemistry, electronic spectroscopy and ESR of the mixed ligand redox series, $[RuN_4LL]^{n+}$, where N_4 = bis-2,2'-bipyridine (bpy) or tetrakis-pyridine (py) and LL = orthophenylene ligand.

Specific abbreviations for complexes are shown in the Experimental section. Thus bpy(nn)qH_2 refers to the bipyridine ruthenium(II) complex containing the orthophenylenediamine ligand in its quinone oxidation state, while (no)catH_2 would refer to complexes of the aminophenol ligand, in its catechol oxidation state, where no distinction is drawn between pyridine or bipyridine bound ruthenium. The labels (oo), (no) and (nn) will be used to designate complexes of these orthophenylene ligands where no distinctions are made between the pyridine and bipyridine bound species, nor between oxidation state.

Our spectroscopic data for bpy(nn)qH_2 agree with data in a previous report.[23] We differ, however, in reporting reversible or quasi-reversible electrochemistry for this species which had previously been reported to display highly irreversible electrochemistry.

Experimental

Reagents

All solvents and reagents used for synthetic purposes were reagent grade or better and used as purchased except where otherwise stated. Orthophenylenediamine (BDH) was recrystallized from benzene, and cobaltocene (Strem) was sublimed, before use. Aldrich Gold Label acetonitrile (MeCN), BDH dichloroethane (DCE), and Aldrich 2-Methyl-tetrahydrofuran (MeTHF) were distilled from P_2O_5, CaH_2, and sodium, respectively. Tetrabutylammonium perchlorate (TBAP) and tetrabutylammonium hexafluorophosphate (Kodak; TBAH) were recrystallized from absolute ethanol and dried under vacuum at 100°C for 24 hrs. Benzoyl peroxide (BDH) was dried at 100°C for 24 hrs before use.

Physical Measurements

Spectroscopic measurements were recorded on the following instruments: UV/VIS spectra - Hitachi Perkin-Elmer Model 340 microprocessor spectrophotometer or a Varian Cary 2400 spectrophotometer; ESR spectra - Varian E4 Electron Spin Resonance Spectrophotometer (X-band; 77K in frozen solutions of DCE or MeTHF). Photoelectron (PES) data were recorded in the Surface Science Laboratory of the University of Western Ontario. Binding energies are relative to C(1s) at 285.0 eV with an estimated error of ±0.3 eV.

Cyclic voltammetry (CV) was performed in 0.1 M TBAP or TBAH solutions in either DCE or acetonitrile on Princeton Applied Research Models 173, 174, and 175, instrumentation. Platinum wires served as counter and working electrodes against a non-aqueous AgCl/Ag (-0.037 V vs. SCE) reference electrode. The potentials are reported vs SCE.

Bulk electrolysis and spectro-electrochemistry were performed in a 1 cm glass cuvette using a platinum gauze working electrode, nichrome wire counter electrode (separated from solution by a frit), and a non aqueous AgCl/Ag reference electrode. Nitrogen gas, saturated with solvent, was continuously bubbled through the cell to provide both mixing and an inert atmosphere.

All syntheses were performed under nitrogen except where otherwise stated. The CHN microanalyses were performed by the Canadian Microanalytical Service, Vancouver.

Preparation of Complexes

$[Ru(bpy)_2(nn)catH_4](PF_6)_2$ = bpy(nn)catH$_4$

A mixture containing ethanol (6 mL), anhydrous $Ru(bpy)_2Cl_2$[37] (0.102 g, 0.22 mmol.), and orthophenylenediamine (0.025 g, 0.23 mmol) was refluxed for 4 hrs during which time a red solution formed. The solution was cooled to room temperature and acidified with 1:10 acetic acid:ethanol (0.2 mL). A solution of NH_4PF_6 (0.3 g) in water (10 mL) was added to the solution. The mixture was boiled until all of the resulting precipitate dissolved. The solution was cooled slowly to room temperature during which time orange-red crystals formed. The crystals were isolated by filtration in air, washed with 2% acetic acid, copious amounts of ether and hexanes and air dried. (Yield: 0.14 g; 81%.) PES Ru $3d_{5/2}$ 280.8 eV.

Anal: Calc'd. for $C_{26}H_{24}N_6P_2F_{12}Ru$: C,38.48; H,2.98; N,10.36. Found: C,38.29; H,2.92; N,10.20%.

$[Ru(bpy)_2(nn)sqH_2](PF_6)$ = bpy(nn)sqH$_2$

For spectroscopic purposes, this material was prepared by the addition of an excess of bpy(nn)qH$_2$ to a dilute solution of cobaltocene in MeTHF. The resulting blue solution which contains the PF_6^- salts of the desired complex and the cobalticenium ion, was decanted from the unreacted bpy(nn)qH$_2$ which remained insoluble in MeTHF. The product showed electronic and

ESR spectra that were identical to those obtained by the electrochemical reduction of bpy(nn)qH_2 at a potential slightly negative of the first reduction wave. The compound was not isolated because of its reactivity towards oxygen and water. The cobaltocenium ion present in the reaction mixture did not significantly interfere with the electronic spectrum because of its relatively low extinction coefficient.

$[Ru(bpy)_2(nn)qH_2](PF_6)_2$ = bpy(nn)qH_2

This compound was synthesized using a modified procedure of Zelewsky[23] as follows. A saturated solution of bpy(nn)$catH_4$ in conc. ammonia/acetone/water (1:5:4), was bubbled with air for 3.5 hrs during which time the red color deepened. The solution was flash evaporated to dryness and the residue was redissolved in a minimum amount of boiling water to which were added ten equivalents of NH_4PF_6. Subsequent slow cooling to room temperature gave copper colored crystals of product which were isolated by filtration, rinsed with sparing amounts of cold water followed by copious amounts of ether and hexanes, and air dried. (Yield: >80%.) PES Ru $3d_{5/2}$ 281.4 eV. Anal: Calc'd. for $C_{26}H_{22}N_6P_2F_{12}Ru$: C,38.57; H,2.77; N,10.38. Found: C,38.78; H,2.90; N,10.10%.

$[Ru(py)_4(nn)qH_2](PF_6)_2$ = py(nn)qH_2

Silver nitrate (0.070 g, 0.41 mmol) was added to a suspension of trans-$Ru(py)_4Cl_2$[38] (0.10 g; 0.21 mmol) in methanol. Stirring was maintained for 30 min after which the precipitated AgCl was removed by filtration through Celite. To the filtrate was added solid orthophenylenediamine (0.022 g 0.21 mmol) and after stirring for 30 min, the orange solution was bubbled with air for an hour during which time the solution became purple. A 1% solution of NH_4PF_6 (10 mL) was added to the solution which was subsequently concentrated until the product began to precipitate. The product was redissolved by heating, and reprecipitated by slow cooling to -15°C. The resulting crude product was isolated by filtration and purified by soxhlet extraction with DCE. Crystals were obtained by slowly diffusing diethyl-ether into the extract. (Yield: 50%) Anal: Calc'd. for $C_{26}H_{26}N_6P_2F_{12}Ru$: C,38.38; H,3.22; N,10.83. Found: C,37.71; H,3.39; N,10.01%.

$[Ru(py)_4(nn)sqH_2](PF_6)$ = $py(nn)sqH_2$

For spectroscopic purposes, blue-green solutions of this compound were chemically generated in the same manner as $bpy(nn)sqH_2$. However, it was harder to generate this compound electrochemically than the bipyridine analogue since a steady state current was approached, indicating that the solvent (DCE or acetonitrile) was catalytically reduced by the compound.

$[Ru(py)_4(nn)catH_4](PF_6)_2$ = $py(nn)catH_4$

For spectroscopic purposes, yellow solutions of this compound were generated by reducing $py(nn)qH_2$ with zinc amalgam in 10% aqueous acetic acid solutions or by bulk electrolysis in the same medium at -0.36 V vs. SCE. The product gave the same electronic spectrum as the reaction mixture used to prepare $py(nn)qH_2$ but prior to air oxidation. This complex oxidizes in air at a moderate rate.

$[Ru(bpy)_2(no)catH_2](ClO_4)$ = $bpy(no)catH_2$

To a suspension of $Ru(bpy)_2Cl_2$ (0.1 g; 0.21 mmol) in methanol (5 mL) was added silver nitrate (0.069 g; 0.21 mmol) in methanol (5 mL). After 30 minutes of stirring, the precipitated AgCl was removed by filtration through Celite. Methanolic triethylamine (10%; 0.21 mmol; 0.29 mL) followed by 2-aminophenol (0.025 g; 0.23 mmol) in methanol (5 mL) were added dropwise to the filtrate while stirring. The resulting blood-red solution was refluxed for 30 min and then reduced in volume to 5 mL by passing N_2 over the hot solution. Lithium perchlorate trihydrate (0.036 g; 0.23 mmol) in methanol (2 mL) was added to the hot reaction mixture. The mixture was cooled to room temperature and toluene/diethyl ether (2:1; 65 mL) was gently added to the quiescent solution. The mixture was allowed to sit overnight during which time cubic, black crystals were deposited. The product was collected by filtration and washed with copious amounts of toluene and hexanes. (Yield: >80%). Anal: Calc'd. for $C_{26}H_{22}N_5O_5ClRu$: C,50.28; H,3.57; N,11.28%. Found: C,52.15; H,3.84; N,11.96%.

$[Ru(bpy)_2(no)sqH]^+$ = $bpy(no)sqH$ and $[Ru(bpy)_2(no)qH]^{2+}$ = $bpy(no)qH$

These species were generated from dilute DCE solutions of $[Ru(bpy)_2(no)catH_2](ClO_4)$ by the stoichiometric addition of benzoyl peroxide. The semiquinone complex is brown in solution

while the quinone complex is purple. Although these species were not isolated, the reactions were reversible by the addition of methanolic ascorbic acid solutions, indicating that the oxidation processes did not decompose the complexes.

$Ru(bpy)_2(oo)cat$ = bpy(oo)cat

The synthesis of this compound and its redox isomers is described elsewhere.[7,8]

$[Ru(py)_4(oo)sq](PF_6)$ = py(oo)sq

To a stirred mixture of t-$Ru(py)_4Cl_2$ (0.1 g, 0.21 mmol) and catechol (0.023 g, 0.205 mmol) in deoxygenated methanol (30 mL), was added a methanolic solution of sodium hydroxide (2 mL, 0.2 M). This mixture was refluxed for 16 hrs during which time the $Ru(py)_4Cl_2$ dissolved giving, initially, a blood-red solution and then a brown solution. The solution was exposed to air, filtered, and allowed to cool. During this process, the color of the solution changed to green. After cooling to room temperature, a solution of NH_4PF_6 (0.1 g) in water (2 mL) was added. The solution was allowed to stand at room temperature for five days, thereby yielding dark green crystals of py(oo)sq.$2H_2O$ (0.52 g, 36%). These were collected by filtration, washed with methanol:water 2:1, diethyl ether, and air dried. Anal Calc'd. for $C_{26}H_{28}N_4O_4PF_6Ru$: C,44.19; H,3.99; N,7.93. Found: C,44.09; H,3.48; N,8.25%.

$Ru(py)_4(oo)cat$ = py(oo)cat and $Ru(py)_4(oo)q(PF_6)_2$ = py(oo)q

These compounds were easily obtained by bulk electrolysis in DCE solutions of py(oo)sq, at -0.4 V and 0.8 V vs. SCE, respectively. The reduced species is bright yellow in dilute solutions while the oxidized species is green-blue.

Attempted syntheses

$[Ru(py)_4(no)catH_2](PF_6)$ = py(no)$catH_2$

Attempts to synthesize this compound by procedures similar to those used in the other orthophenylene ligand complexes produced a yellow, unidentified compound. Thus, the redox series of this complex could not be obtained.

Deprotonated Species

Attempts were also made to characterize deprotonated forms of the bpy(nn) and (no) catechol complexes to maintain constant the number of protons within each orthophenylene ligand group. Such deprotonated species are stable in high oxidation state rhenium and osmium complexes,[32] however, we were quite unable to obtain these species in our ruthenium(II) series either by electrochemical or chemical methods. Electrochemical polarization slightly negative of the second reduction couple of bpy(nn)qH_2 in aprotic media generated what appeared to be a mixture of bpy(nn)sqH_2 and bpy(nn)catH_4. The current reached a steady state due to catalytic solvent reduction. Removal of the applied potential from the cell caused the majority of species in solution to be rapidly oxidized to bpy(nn)sqH_2, in spite of the inert atmosphere.

Attempts to chemically reduce bpy(nn)qH_2 by two electrons using sodium amalgam in propylene carbonate solution initially generated bpy(nn)sqH_2, after which a yellow decomposition product irreversibly formed. Deprotonation of bpy(nn)catH_4 using several strong bases including sodium methoxide in methanol solution, sodium amide suspension in pyridine, and lithium aluminum hydride suspension in THF (this required the use of the 4,5-dimethylated orthophenylenediamine complex for solubility reasons), initially formed what was determined by electronic and ESR spectroscopy to be bpy(nn)sqH_2. The latter two reactions further produced a species whose electronic spectrum resembled bpy(nn)qH_2. Since all of the color changes developed at the interface between the solution and the particles of base, leakage of oxygen into the air-sensitive system could be ruled out as a cause of the apparent oxidations.

Results and Discussion

Electrochemistry

The cyclic voltammograms of the orthophenylene ligand complexes show multiple couples which result from redox processes centered at the metal, the orthophenylene ligand, and the bpy ligands. Using arguments discussed previously,[7] one may assign these couples as shown in Table I.

With the exception of bpy(nn)catH_4 and bpy(no)catH_2, the cyclic voltammograms of the orthophenylene complexes, in an organic solvent, show two chemically reversible orthophenylene ligand couples which shift negatively as oxygen donors are replaced by the more electron rich nitrogen atoms on the orthophenylene ligand (Table I). (Figure 1). The bpy(nn)catH_4 and bpy(no)catH_2 complexes show a chemically irreversible two-electron oxidation wave attributed to the concomitant irreversible loss of a hydrogen atom from each orthophenylene ligand nitrogen atom during the oxidation of the ligand from the catechol to quinone form (Figure 2).

Once these protons are lost, then the partially deprotonated species on the electrode display reduction waves on the return scan at potentials coinciding with the ligand redox couples of the bpy(no)qH and bpy(nn)qH_2 complexes. These waves are scan rate dependent, increasing in size relative to the ruthenium and bipyridine redox couples as the scan rate is increased. They are assigned to reductions of the orthophenylene ligand in the bpy(no)qH and bpy(nn)qH_2 species generated during the anodic scan.

Spectroelectrochemistry shows that bpy(no)catH_2 is oxidized to bpy(no)qH prior to the metal oxidation; thus, the metal oxidation that is observed in the cyclic voltammogram of bpy(no)catH_2 actually belongs to bpy(no)qH and is reported as such. New reduction waves observed in the electrochemically generated bpy(no)qH have been assigned to the bpy(no)qH redox couples. A similar situation exists in the bpy(nn) complexes. Here, bpy(nn)catH_4 and bpy(nn)qH_2 which were separately isolated show, within experimental error, the same Ru(III)/Ru(II) potential. Bulk electrolysis at the orthophenylene ligand oxidation wave of bpy(nn)catH_4 similarly produces bpy(nn)qH_2 as shown spectroscopically, and new reduction waves are observed which have potentials coincident with the ligand redox potentials of the isolated bpy(nn)qH_2. The complexes all contain the ruthenium(II) center with the dioxolene being sequentially oxidized to quinone, but see discussion below. Data are collected in Table I.

ESR Spectroscopy

The ESR spectra of the semiquinone complexes (Figure 3) show signals centered around g = 2, indicating the presence of a ligand centered radical. The successive replacement of orthophenylene ligand oxygen atoms with nitrogen results in a slight narrowing of the ESR signal {bpy(oo)sq, δpp (peak to peak separation, between main estrema) = 105 G ; bpy(no)sqH, δpp = 82 G; bpy(nn)sqH_2, δpp = 75 G; for conditions see legend to Figure 3} the appearance of nitrogen hyperfine structure, and the decrease of the g value below that of a free radical {bpy(oo)sq, 2.000; bpy(no)sqH, 2.000; bpy(nn)sqH, 1.997}. The lowering of the g value below that of a free radical is typical of a ligand-centered radical complex containing a ruthenium bis(bipyridine) fragment, where the empty bpy-π^* orbitals are of slightly higher energy to those of the radical ligand.[39]

Electronic Spectroscopy

The electronic spectra (Table II) of the orthophenylene ligand complexes were assigned, as discussed in depth previously,[7] by making comparisons between the bpy complexes and their py analogues and by observing peak shifts caused by both changes in the oxidation state of the complexes, and changes in the orthophenylene ligand.

The electronic spectra and other characteristics of the orthophenylene ligand complexes can be explained by the qualitative molecular orbital (MO) diagram shown in Figure 4. The Gordon and Fenske ligand orbital symmetry labels have been maintained, for discussion of mainly ligand based orbitals, for ease of comparison with the literature; they apply to the C_{2v} local ligand symmetry,[40] however, it is also acceptable to assign the resulting molecular orbitals in the effective C_{2v} microsymmetry of the central metal. Thus, the metal d_{xy} and d_{yz} orbitals interact with the orthophenylene ligand $2a_2(\pi)$ and $3b_1(\pi^*$-LUMO) orbitals in weak and strong π-interactions respectively, while the d_{z2} and d_{xz} orbitals interact with the orthophenylene ligand $9a_1$ and $7b_2$ orbitals in weak and strong σ-interactions respectively. The d_{x2-y2} orbital remains non-bonding with respect to the orthophenylene ligand but is strongly destabilized by σ-bonding with the bipyridine ligands.

The salient features of the π-interaction (Figure 4) then are the formation of a pair of

orbitals, b_2 and $2b_2^*$ being the bonding and anti-bonding combinations of the metal d_{yz} and ligand $3b_1$ orbitals (local symmetry label); as will be discussed below, transitions between these two orbitals are a dominant feature of the electronic spectra of these species.

The relative arrangement of the bpy and orthophenylene ligand based π^*-MO energies is supported by electrochemical data and by the ligand-centeredness of the semiquinone complex ESR signals, which originate from an unpaired electron residing in the semiquinone π^*-MO.

a) Catechol Complexes

The catechol complexes are unambiguously ruthenium(II) species comprised of fully reduced orthophenylene ligands which offer no low lying energy levels to which MLCT transitions can occur. This is also confirmed by the ruthenium $3d_{5/2}$ core photoelectron spectrum (see experimental) of bpy(nn)CatH_4, which is consistent with ruthenium(II).[41-48]

All of the intense visible region absorptions must therefore originate from MLCT transitions to either the bpy or py π^*-orbitals or from π ---> π^* intraligand transitions. These latter transitions are high in energy and occur in the UV region.[49] Thus, the bands observed in the visible spectra of the bpy complexes, covering the region from 16,000 - 21,000 cm^{-1} (Figure 5a), are assigned to the Ru ---> π^*(1) bpy transitions while those lying approximately 8,500 cm^{-1} higher in energy are assigned to Ru ---> π^*(2) bpy transitions (referring respectively to the LUMO and SLUMO orbitals on the bipyridine ligand). The strongest band in the visible spectra of the py complexes (Figure 6a) is assigned to the Ru ---> py π^*(1) transition.

The MLCT transitions to bipyridine (or pyridine) shift to higher energies as the number of nitrogen donors on the orthophenylene ligand increases (Figure 7); this is a direct consequence of the change in net charge on these ligands, from (-2) to (0), respectively, caused by the additional protons on the coordinating nitrogen atoms.

These transitions are relatively broad, due to the ligand field splitting of the metal d-orbital energies, and ligand-ligand interaction. While the (oo)cat complexes carry no protons, it is possible to protonate these species in-situ by addition of trifluoroacetic acid. This causes a shift to higher energy of the Ru ---> π^*(1) bpy transition. Both the protonated pyridine and bipyridine

catechol complexes exhibit Ru ---> py/bpy charge transfer bands at energies that are slightly lower than those of the bpy(no)catH_2 complexes, suggesting that the protonated species are singly protonated since double protonation should yield a higher charge transfer energy than in the bpy(no)catH_2 complexes.

The spectra of the (oo)cat and (no)catH complexes are complicated by broad, ill-resolved, interligand charge transfer (LLCT) bands, which involve transitions from the lone pair orbitals of the orthophenylene ligand oxygen atoms to the π^* orbitals of bpy or py (Table II). Preliminary resonance Raman data for bpy(no)catH_2 supports this assignment to a LLCT transition.[50] Such transitions do not occur from nitrogen donor atoms since these pairs are bound to hydrogen. The transitions are expected to be relatively weak, because of poor overlap, and relatively broad, because of a significant reorganization contribution.

Using methods[51] based upon the observed oxidation and reduction potentials of the bpy(oo)cat complex, the $3b_1$ (cat) ---> π^*(1) bpy transition can be calculated to lie at approximately 11,200 cm^{-1} exclusive of reorganization energy, which is then estimated to be about 2500 cm^{-1}. One might have expected the corresponding transition in bpy(no)catH_2 to lie at lower energies since nitrogen is less electronegative than oxygen. It does not do so because of the protons present on the nitrogen atom. It would lie lower in the deprotonated bpy(no)cat species which we have not been able to isolate (see Expt.).

When the bpy(oo)cat complexes are singly protonated with trifluoroacetic acid in DCE solutions the LLCT bands vanish and the spectra become strikingly similar to the spectra of bpy(nn)catH_4 and py(nn)catH_4 complexes (Figure 8). Attempts to doubly protonate bpy(oo)cat led to the decomposition of the complex while several-fold excess of acid added to py(oo)cat did not further change the spectrum of the monoprotonated species.

Since the catechol ligands are electron rich, and readily oxidisable, one might expect to see LMCT transitions from catechol oxygen electron pairs to the empty d_{xz} and $d_{x^2-y^2}$ orbitals on Ru^{II} (see Figure 4 for coordinate scheme). No evidence for these transitions was seen. They may be expected to contribute to absorption above 30,000 cm^{-1}, but will be weak due to overlap

constraints.

b) Semiquinone Complexes

The ESR spectra of these species show that the unpaired electron is located primarily on the semiquinone ligand and therefore that the proper description of these species is ruthenium(II) semiquinone. On the other hand, the analogous osmium (oo) complex[52] has a dramatically different ESR spectrum, characteristic of osmium(III) and therefore an Os(III)(oo)(cat) electronic structure.

The electronic spectra of the ruthenium(II) semiquinone complexes (Figures 5b and 6b) are dominated by an intense absorption at low energies ($\log(\epsilon) = 3.9 - 4.3$; $E_{op} = 10{,}500 - 16{,}000$ cm^{-1}), assigned previously to a MLCT to the orthophenylene ligand whose half-filled $3b_1$ π^*-orbital ($2b_2^*$ in the MO scheme in Figure 4) is now accessible. This transition dramatically shifts to higher energies with the number of nitrogen donor atoms. In a related series of complexes with 4,5-disubstituted-1,2-diiminobenzene ligands, to be reported in detail elsewhere,[53] this transition shifts very significantly to the red with electron withdrawing substituents, confirming strong MLCT character.

The Ru ---> bpy charge transfer bands, which are centered around 20,000 cm^{-1} (Ru ---> π^*(1) bpy) and 29,000 cm^{-1} (Ru ---> π^*(2) bpy), shift little with changes in the number of nitrogen donors in the orthophenylene ligand (Figure 7) and are easily distinguished from the Ru ---> orthophenylene ligand (a_2, b_2 ---> $2b_{2*}$) band due to their lower extinction coefficients ($\log(\epsilon) = 3.6 - 4.0$) and irregular band shapes (Table II).

The spectra of the semiquinone complexes are complicated by both inter- and intra-ligand transitions whose assignments[54] are tentative (Table II). The $2a_2$ ---> $3b_1$ intraligand transition, which is centered in the near UV region in free semiquinone[55] as well as in Zn(II) and Ni(II) complexes[16], probably accounts for the absorptions near 26,200 and 23,000 cm^{-1} in the bpy(no)sqH and bpy(nn)sqH_2 species, respectively. This absorption is probably obscured by the Ru ---> π^*(2) bpy band in the bpy(oo)sq species.

The energies of the $3b_1$ (sq) ---> π^* bpy LLCT bands can be estimated from the

electrochemical potentials[56] as noted above. Using data in Table I, this transition, in bpy(oo)sq, is predicted to lie near 18,400 cm^{-1} exclusive of a reorganization contribution. The broad band near 20,000 cm^{-1} likely contains this band. Although py(nn)sqH_2 also appears to exhibit a weak transition around 18,700 cm^{-1} this is probably due to residual py(nn)qH_2 present from the synthesis of the complex.

There are broad near infrared absorptions of very low intensity in both the bpy(nn)sqH_2 and bpy(no)sqH complexes at 11,000 cm^{-1} and 12,000 cm^{-1}, respectively whose provenance is unknown. They may be spin forbidden CT bands, or $2b_2$ ---> π^* (1) bpy, or internal n ---> π^* sq

c) Quinone Complexes

An X-ray structure of (bpy)(nn)qH_2 shows[23] C=N bond lengths typical of a quinonoid ligand, implying therefore a ruthenium(II) formulation. The Ru $3d_{5/2}$ core photoelectron spectra (see experimental) are in the border region, high but not unacceptable for Ru(II) and low, but possible, for Ru(III).

The quinone complexes exhibit an intense electronic absorption at E_{op} = 15,600 - 19,400 cm^{-1}, ($\log(\epsilon)$ = 3.76 - 4.34) which shifts to higher energy as the number of nitrogen donors on the orthophenylene ligand increases (Figures 5c and 6c; Table II). This absorption has also been previously assigned to a Ru ---> $3b_1$ (b_2 ---> $2b_2^*$) MLCT transition.[7]

The transitions are broader than the corresponding Ru ---> sq transitions (vide infra). In the aforementioned study of complexes with 4,5-disubstituted-1,2-diiminobenzene ligands,[57] this transition, in the quinone complexes, does not shift regularly with electron withdrawing substituents, and the magnitude of the shift is half that observed for the semiquinone species discussed above. The small shifts are, however, more reconcilable with an LMCT transition than with an MLCT transition. The corresponding Ru ---> quinone transition in $Ru(NH_3)_4$(oo)q occurs at[57] 19,500 cm^{-1} significantly higher in energy than observed in the bipyridine analogue. Since the $Ru(NH_3)_4$ fragment is certainly easier to oxidise than the $Ru(bpy)_2$ fragment, this observation would again be consistent with an LMCT transition rather than an MLCT transition.

The Ru ---> quinone transitions in $[Ru(bpy)_2RBQ]^{2+}$ occur[7] at 14,950 cm^{-1} with RBQ =

3,5-di-t-butyl-1,2-benzenequinone and at 15,650 cm^{-1} with RBQ = 3,4,5,6-tetrachloro-1,2-benzenequinone, compared with 15,600 for bpy(oo)q. The lack of a shift upon chlorine substitution suggests little charge transfer character while the blue shift with the more electron donating t-butyl substituted species is again more reconcilable with a LMCT than MLCT transition. Resonance Raman data, exciting into the Ru ---> quinone (b_2 ---> $2b_2^*$) transition of bpy(oo)q, revealed vibrational enhancements consistent with little charge transfer character.[8] These observations bring into question whether this transition should, in fact, be represented Ru ---> quinone or rather semiquinone ---> Ru. We return below to further consideration of these observations and, to avoid misrepresentation, refer henceforth to this transition as Ru/quinone.

The Ru ---> π^*(1) bpy band appears at higher energies and with lower intensity than the Ru/quinone transition. This Ru ---> π^*(1) bpy band shifts slightly to lower energies with replacement of the oxygen atoms of the orthophenylene ligand by nitrogen (Figure 7). In contrast to the behaviour of the catechols (vide supra) it is now the more electron rich (nn) species, in these neutral quinones, placing charge onto the metal atom, which shifts the Ru ---> π^* bpy transition to lower energy. An internal orthophenylene ligand transition may occur at similar energies.

Energy Matching, Ruthenium-Ligand Orbital Mixing, and Reorganization Energies

The degree of orbital mixing, specifically in the b_2 and $2b_2^*$ orbitals, will depend upon the matching of orbital and metal energies, and the extent of (symmetry permitted) overlap.

An experimental measure of the mixing can be obtained through analysis of the reorganization energies involved in the b_2 ---> $2b_2^*$ transitions. A transition from a metal localized orbital to a ligand localized orbital should exhibit significant reorganization energy, with strong charge transfer character, especially as the bond distances in these orthophenylene ligands are very dependent upon their net oxidation state. A small reorganization energy signals a transition between largely mixed metal-ligand orbitals,[58] and, in our systems, with little charge transfer character.

Reorganisation energies may be estimated, in a relative sense, from the halfbandwidths of

the relevant transitions.[59] However, of the two possible observable transitions, one, b_2 ----> $2b_2^*$, is strongly allowed, and the other a_2 ---> $2b_2^*$ is allowed but with poor overlap;[60,61] both will occur within the same band envelope. The a_1 ---> $2b_2^*$ transition would vanish through overlap orthogonality. The bandwidth must, therefore, reflect the degree of splitting between the b_2 and a_2 metal orbitals. The extent of such splitting will depend upon the true symmetry, and on differences between the π-interactions of the bipyridine and orthophenylene ligands.

The bpy(nn) and py(nn) species have a RuN_6 pseudo-octahedral symmetry and the (oo) species, while technically C_2, has a pseudo-D_{4h} splitting pattern; both these point groups, if they rigorously applied would make the a_2 and b_2 orbitals degenerate. Thus, both these species are of relatively high symmetry. On the other hand, the (no) species can only possess C_1 symmetry. On this basis, the splitting of the CT bands should be greatest in the (no) species, and this is seen to be the case (Table III).

Specifically for the (nn) and (oo) species, the relative reorganization energies may be compared directly by considering the halfbandwidths of the transitions in the semiquinone and quinone species (Table III).

For a given orthophenylene ligand, the Ru ---> sq MLCT transitions are narrower than the Ru/quinone transitions. For the quinone oxidation state, the Ru/quinone band is narrowest in the species bpy(nn)qH_2, and for the semiquinone oxidation state, the Ru ---> $3b_1$ (b_2 ---> $2b_2$) semiquinone transition in bpy(oo)sq is slightly narrower than in bpy(nn)sqH_2 but there is little difference (Table III).

The observation that the bpy(nn)qH_2 complex Ru/quinone transition has a narrower band than that in the bpy(oo)q complex, yet lies at higher energy, is very unusual. Generally speaking bands of similar origin become broader as they shift to higher energies.[59,61]

a) **Electronic Structure of the Semiquinone Species.**

Thus, in view of the very narrow Ru ---> sq (b_2 ---> $2b_2^*$) transitions, the degree of mixing between metal d_{yz} and semiquinone ligand $3b_1$ (see Figure 4) (in b_2 and $2b_2^*$) is considerable and a little more important in the (oo) series than in the (nn) series because of better energy matching.

Overlap terms may be comparable for the three negatively charged semiquinone ligands.

The resulting $2b_2^*$ LUMO, containing the unpaired electron, has greater ligand character in the (nn) series than in the (oo) series, fully consistent with the observed electron spin resonance data.

The oscillator strengths of the Ru ---> sq MLCT band are quite large (Table II), slightly more so for the (oo)sq species than for the (nn)sqH_2 species. The combination of narrower band and higher oscillator strength is particularly significant. Since intensity arises from $\langle L | r | L \rangle$ matrix elements,[61,62] such an observation also indicates a greater degree of mixing for the bpy(oo)sq species relative to bpy(nn)sqH_2.

b) Electronic Structure of the Quinone Species.

In the quinone oxidation state, we propose that such metal/ligand mixing, in the b_2 and $2b_2^*$ orbitals, is significantly better for the (nn) series than for the (oo) series, and greater than in the semiquinone series. Overlap, and hence mixing, will also be better in the (nn) series than in the (oo) series because of the greater electron richness of the former as indicated by the shift in the Ru ---> π^* bpy transition, noted above (Figure 7).

This proposal leads to the conclusion that the b_2 orbital will have more ligand character in the (nn) series than in the (oo) series, and therefore the, now empty, anti-bonding combination (LUMO) will have more metal character in the (nn) series than in the (oo) series.

This supposition explains the very narrow Ru/quinone transition in bpy(nn)qH_2 relative to that in bpy(oo)q (and similar but less dramatic observation in the pyridine analogues). There is greater mixing of the orbitals and less charge transfer character of the transition in the (nn) series (c.f. resonance Raman data cited above). This also explains why these transitions, to the extent that they do have charge transfer character, are ill behaved demonstrating characteristics of both MLCT and LMCT transitions. The shift to higher energy for the Ru/Q transition in these quinones relative to the corresponding band in the semiquinones arises from the strong overlap stabilisation. This problem is addressed in more detail elsewhere.[53]

Note that the strong interaction proposed between the d_{yz} metal orbital, and ligand $3b_1$

orbital is equivalent to describing a π-backbonding interaction between metal and quinone ligand. This is supported by the X-ray structural study[23] of $[Ru(II)(bpy)_2(nn)qH_2](PF_6)_2$ demonstrating that the Ru-N(diimine) bond (2.02 Å) was substantially shorter than the Ru-N(bipyridine) bond (2.08 Å) which fact was attributed to significant π-back donation to the diimine ligand.

In parallel with the observation reported above for Ru(oo)sq, the oscillator strength for the Ru/quinone transition is at a maximum for the bpy(nn)qH_2 species, consistent with greater mixing therein. The extra mixing, and presumable stabilization of the quinonediimine species may also explain why many quinonediimine ruthenium complexes have been reported in the literature, but few, if any, quinone ruthenium(II) species have been isolated.

Although these complexes are described here as ruthenium(II) quinone derivatives, it is pertinent, in the light of the above discussion, to ask whether they should indeed be so described. A strong interaction between metal d_{yz} and ligand $3b_1$ orbitals, with the b_2 orbital being more ligand-like and containing two electrons, leads to the formal description $[Ru(III)(bpy)_2(semiquinone)]^{2+}$, if weighted electron populations are summed (assuming the b_2 orbital to be 50:50 M:L). Such a discussion of apparent oxidation state is reminiscent of early work by tom Dieck[59,63] on molybdenum phosphine carbonyl species which behave in an analogous fashion, and of similar discussions by Meyer.[37,42,64] The report is also relevant to earlier studies of the effect of metal-ligand mixing on charge transfer energies and effective oxidation states by Taube,[65,66] Creutz,[67] and Kaim.[68]

Certainly one may suppose that there is such a Ru^{III} contribution to the description in a valence bond sense, a contribution which is, indeed, consistent with the PES data (Expt.).[42-48]

However the X-ray data (quoted above) are appropriate for Ru^{II}, and the Ru ---> bpy transitions are typical of Ru(II) bipyridine species. The observed Ru ---> π^* (1) bpy transition is consistent[56] with the electrochemical potentials as assigned.

In summary, these quinone complexes are considered to be better described by the Ru(II) description rather than the Ru(III) description, i.e. the b_2 orbital is still centered more on the metal than on the ligand.

The osmium complex, corresponding with (bpy)(oo)q has electronic spectra interpreted[52] in terms of $[Os(III)(bpy)_2(DTBSq)]^{2+}$. Thus the trivalent character is much better expressed in the osmium series, as also observed, for example, in the species $[M(NH_3)_5(N\text{-methylpyrazinium})]^{3+}$. M = Ru, Os.[67]

Conclusions

Our studies have provided information concerning the variation in orbital mixing and metal-ligand bonding as a function of ligand donor in these non-innocent systems. There is extensive orbital overlap in many of these complexes leading to no clear distinction between one oxidation state and another, though ruthenium(II) is the best overall description.

Current complementary studies include X-ray structural analyses of some of these species to provide structural data relating to ground state structure, resonance Raman studies to probe the vibrational coupling in the CT and intra-ligand transitions, and molecular orbital studies to obtain greater insight into the mixing processes involved.

Acknowledgements We are indebted to the Natural Sciences and Engineering Research Council (Ottawa) and the Office of Naval Research (Washington) for financial support. We also thank Dr. Elaine Dodsworth for useful discussion, and the Johnson-Matthey Company for the loan of ruthenium trichloride.

Figures

Scheme 1. The orthophenylene ligand redox isomers.

(nn)catH_4, X = Y = NH_2; (nn)sqH_2 or (nn)qH_2, X = Y = NH;

(no)catH_2, X = NH_2; Y = O; (no)sqH or (no)qH, X = NH; Y = O;

(oo)cat or (oo)sq or (oo)q, X = Y = O; For (nn), n=2; (no), n=1; (oo), n=0

Figure 1. The cyclic voltammograms of the orthophenylene ligand complexes.

a) ca. 10^{-3} M bpy(oo)cat in DCE; 0.1 M TBAH; Scan rate 200 mV/sec.

b) ca. 10^{-3} M bpy(nn)qH_2 in acetonitrile; 0.1 M TBAH; Scan rate 200mv/sec.

Figure 2. The cyclic voltammograms of catechol complexes.

a) ca. 10^{-3} M bpy(no)catH_2 in acetonitrile; 0.1 M TBAH; Scan rate 200 mV/sec.

b) ca. 10^{-3} M bpy(nn)catH_4 in acetonitrile; 0.1 M TBAH; Scan rate 200 mV/sec.

Figure 3. The ESR spectra of the semiquinone complexes at 100 K. a) ca. 10^{-5} M bpy(oo)sq in DCE; b) ca. 10^{-5} M bpy(no)sqH in DCE generated by the oxidation of the bpy(no)catH_2 with benzoyl peroxide; c) ca. 10^{-5} M bpy(nn)sqH_2 in 2-MeTHF generated by the reduction of bpy(nn)qH_2 with cobaltocene.

Figure 4. Simplified molecular orbital diagram of the ruthenium bis-bipyridine semiquinone complexes. The $3b_1$ π^*-orbital HOMO contains one electron. The quinone and catechol complexes have one less and one more electron in this orbital, respectively. Vertical solid lines indicate allowed transitions.

Figure 5. Electronic spectra of ruthenium bis-bipyridine orthophenylene ligand complexes.

a) Catechol ligand oxidation state.

b) Semiquinone ligand oxidation state.

c) Quinone ligand oxidation state.

, catechol series (oo); DCE.

---, o-aminophenol series (no); DCE.

···, orthophenylenediamine series (nn); MeCN.

Figure 6. Electronic spectra of ruthenium tetrakis-pyridine

orthophenylene ligand complexes.

a) Catechol ligand oxidation state.

b) Semiquinone ligand oxidation state.

c) Quinone ligand oxidation state.

, catechol series (oo); DCE.

···, orthophenylenediamine series (nn); DCE.

Figure 7. Optical energy shifts of the Ru ---> π^* (1) bpy MLCT as a function of oxygen donor substitution by nitrogen.

q, quinone oxidation state; sq, semiquinone oxidation state; cat, catechol oxidation state. This graph also closely approximates, in a relative sense, to the variation in Ru(III)/Ru(II) potential as a function of ligand and oxidation state (see text).

Figure 8. Electronic spectra of protonated catechol complexes.,

bpy(oo)catH; (DCE). ···, py(oo)catH_2; (DCE).

References

1. Burns, R. P.; McAuliffe, C. A. Adv. Inorg. Chem. Radiochem. **1979**, 22, 303.
2. Eisenberg, R. Prog. Inorg. Chem. **1970**, 12, 295.
3. McCleverty, J. A. Prog. Inorg. Chem. **1968**, 10, 49.
4. Kessel, S. L.; Emerson, R. M.; Debrunner, P. G.; Hendrickson, D. N.; Inorg. Chem. **1980**, 19, 1170.
5. Buchanan, R. M.; Claflin, J.; Pierpont, C. G. Inorg. Chem. **1983**, 22, 2552.
6. Harmalker, S.; Jones, S. E.; Sawyer, D. T. Inorg. Chem. **1983**, 22, 2790.
7. Haga, M.-A.; Dodsworth, E. S.; Lever, A.B.P. Inorg. Chem. **1986**, 25, 447.
8. Stufkens D. J.; Snoeck Th. L.; Lever A. B. P. Inorg. Chem. **1988**, 27, 935.
9. Lever, A. B. P.; Auburn, P. R.; Dodsworth, E. S.; Haga, M.-A.; Liu, W.; Melnik, M.; Nevin, W. A. J. Am. Chem. Soc. **1988**, 110, 8076.
10. Thompson, J. S.; Calabrese, J. C. Inorg. Chem. **1985**, 24, 3167.
11. Sofen, S. R.; Ware, D. C.; Cooper, S. R.; Raymond, K. N. Inorg. Chem. **1979**, 18, 234.
12. Boone, S. R.; Pierpont, C. G. Inorg. Chem. **1987**, 26, 1769.
13. Espinet P.; Bailey, P. M.; Maitlis, P. M. J. Chem. Soc., Dalton Trans. **1979**, 1542-1547.
14. Pierpont, C. G.; Buchanan, R. M. Coord. Chem. Rev. **1981**, 38, 45.
15. Cooper, S. R.; Koh, Y. B.; Raymond, K. N. J. Am. Chem. Soc. **1982**, 102, 5092.
16. Benelli, C.; Dei, A.; Gatteschi, D.; Pardi, L. Inorg. Chem. **1989**, 28, 1476.
17. Balch, A. L.; Holm, R. H. J. Am Chem. Soc. **1966**, 88, 5201.
18. Baikie, P. E.; Mills, O. S. Inorg. Chim. Acta **1967**, 1, 55.
19. Duff, E. J. J. Chem. Soc. (A), **1968**, 434.
20. Warren, L. F. Inorg. Chem. **1977**, 16, 2814.
21. Reinhold, J.; Benedix, R.; Birner, P.; Hennig, H. Inorg. Chim. Acta **1979**, 33 209.
22. Vogler, A.; Kunkely, H. Angew. Chem., Int. Ed. Engl. **1980**, 19, 221.
23. Belser, P.; von Zelewsky, A.; Zehnder, M. Inorg. Chem. **1981**, 20. 3098.

24. El'Cov, A. V.; Maslennikova, T. A.; Kukuschkin, V. Ju.; Shavurov, V. V. J. Prakt. Chem. **1983**, B325, S27.

25. Pyle A. M. ; Barton, J. K. Inorg. Chem. **1987**, 26, 3820.

26. Thorn, D. L.; Hoffmann, R. Nouv. J. Chim. **1979**, 3, 39.

27. Peng, S.-M.; Chen, C.-T.; Liaw, D.-S.; Chen, C.-I.; Wang, Y. Inorg. Chim. Acta **1985**, 101, L31..

28. Christoph, G. G.; Goedken, V. L. J. Am. Chem. Soc. **1973**, 95, 3869.

29. Hall, G. S.; Soderberg, R. H. Inorg. Chem. **1968**, 7, 2300.

30. Gross, M. E.; Ibers, J. A.; Trogler, W. C. Organometallics **1982**, 1, 530.

31. Zehnder, M.; Loliger, H. Helv. Chim. Acta **1980**, 63, 754.

32. Danopoulos, A. A.; Wong, A. C. C.; Wilkinson, G.; Hursthouse, M. B.; Hussain, B. J. Chem. Soc., Dalton Trans. **1990**, 315.

33. Nemeth, S.; Simandi, L. I.; Argay, G.; Kalaman, A. Inorg. Chim. Acta **1989**, 166, 34. Gross, M. E.; Trogler, W. C.; Ibers, J. A. J. Am. Chem. Soc. **1981**, 103, 192-3.

35. Miller, E. J.; Brill, T. B. Inorg. Chem. **1983**, 22, 2392.

36. Miller, E. J.; Landon, S. J.; Brill, T. B. Organometallics **1985**, 4, 533.

37. Sullivan, B. P.; Salmon, D. J.; Meyer, T. J. Inorg. Chem. **1978**, 17, 3334.

38. Evans, I. P.; Spencer, A.; Wilkinson, G. J. Chem. Soc., Dalton Trans. **1973**, 204.

39. Ernst, S.; Hänel, P.; Jordanov, J.; Kaim, W.; Kasack, V.; Roth, E. J. Am. Chem. Soc. **1989**, 111, 1733.

40. Gordon, D. J.; Fenske, R. F. Inorg. Chem. **1982**, 21, 2907, 2916.

41. Weaver, T. R.; Meyer, T. J.; Adeyemi, S. A.; Brown, G. M.; Eckberg, R. P.; Hatfield, W. P.; Johnson, E. C.; Murray, R. W.; Untereker, D. J. Am. Chem. Soc. **1975**, 97, 3039.

42. Connor, J. A.; Meyer, T. J.; Sullivan, B. P. Inorg. Chem. **1979**, 18, 1388.

43. Feltham, R. D.; Brant, P. J. Am. Chem. Soc. **1982**, 104, 641.

44. Srivastava, S. App. Spec. Rev. **1986**, 22, 401.

45. Geselowitz, D. A.; Kutner, W.; Meyer, T. J. Inorg. Chem. **1986**, 25, 2015.

46. Brant, P.; Stephenson, T. A. Inorg. Chem. **1987**, 26, 22.

47. Shepherd, R. E.; Proctor, A.; Henderson, W. W.; Myser, T. K. Inorg. Chem. **1987**, 26, 2440.

48. Gassman, P. G.; Winter, C. H. J. Am. Chem. Soc. **1988**, 110, 6130.

49. Bryant, G. M.; Fergusson, J. E.; Powell, H. J. K. Aust. J. Chem. **1971**, 24, 257.

50. Stufkens, D. J.; Lever, A. B. P. unpublished observations.

51. Dodsworth, E. S.; Lever, A. B. P. Chem. Phys. Lett. **1985**, 119, 61.

52. Haga, M-A.; Isobe, K.; Boone, S. R.; Pierpont, C. G. Inorg. Chem. **1990**, 29, 3795.

53. Masui, H.; Lever, A. B. P. paper in preparation.

54. Dodsworth, E. S.; Lever, A. B. P. Chem. Phys. Lett. **1990**, 172, 151.

55. Stallings, M. D.; Morrison, M. M.; Sawyer, D. T. Inorg. Chem. **1981**, 20, 2655.

56. Dodsworth, E. S.; Lever, A. B. P. Chem. Phys. Lett. **1986**, 124, 152.

57. Pell, S. D.; Salmonsen, R. B.; Abelleira, A.; Clarke, M. J. Inorg. Chem., **1984**, 23, 385.

58. The converse is not necessarily true, i.e. transitions between highly mixed states do not always lead to narrow transitions.

59. Renk, I. W.; Dieck, t. D. Chem.Ber. **1972**, 105, 1403.

60. Balk, R. W.; Stufkens, D. J.; Oskam, A. Inorg. Chim. Acta. **1979**, 34, 267.

61. Lever, A. B. P. Inorganic Electronic Spectroscopy, 2nd Edition, Elsevier, Amsterdam, 1984.

62. Desjardins, S. R.; Penfield, K. W.; Cohen, Su. L.; Musselman, R. L.; Solomon, E. I. J. Am. Chem. Soc. **1983**, 105, 4590.

63. tom Dieck, H.: Renk, I. W. Angew. Chem. Int. Ed. Engl **1970**, 9, 793; tom Dieck, H.; Renk, I. W. Chem. Ber. **1971**, 104, 110.

64. Sullivan, B. P.; Salmon, D. J.; Meyer, T. J., Inorg. Chem. **1978**, 17, 3334;

65. Magnuson, R. H.; Taube, H. J. Am. Chem. Soc. **1975**, 97, 5129.

66. Wishart, J. F.; Bino, A.; Taube, H. Inorg. Chem. **1986**, 25, 3318.

67. Creutz, C.; Chou, M. H. Inorg. Chem. **1987**, 26, 2995.

68. Kaim, W.; Gross, R. Comments in Inorg. Chem. **1988**, 7, 269.

Table I. Electrochemical Potentials (Volts) of RuN_4L complexes, where N_4=bis-bipyridine/tetra-pyridine and L=orthophenylene ligand.

Species	Ru(III)/Ru(II)	L/L^{2-}	bpy/bpy$^-$(1)	bpy/bpy$^-$(2)
bpy(nn)catH_4	1.37[a]	0.99[b,a]	-1.58[c]	-1.83[b,a]
bpy(no)catH_2	1.48[a]	0.34[b,a]	-1.56[a]	-1.80[a]

	Ru(III)/Ru(II)	L/L^-	L^-/L^{2-}	bpy/bpy$^-$(1)	bpy/bpy$^-$(2)
bpy(oo)q[d]	1.65[a]	0.56	-0.33	-1.72	
py(oo)q	1.52[a]	0.59	-0.34		
bpy(nn)qH_2	1.35	-0.47	-1.15[c]	-1.72[c]	-1.96[c]
py(nn)qH_2	1.33[c]	-0.48	-1.24		
bpy(no)qH	1.48[e]	0.05[e]	-0.70[e]		

Note: The semiquinone complexes as well as (oo)cat complexes generate cyclic voltammograms with potentials identical to those of their respective quinone form. Solvent = acetonitrile; [$TBAPF_6$] = 0.1M; [complex] = $1x10^{-3}$M. The labels (1), (2) on the bipyridine potentials refer to reduction of the first and second bipyridine unit. a) Chemically irreversible, at scan rate 200 mV/sec. b) peak potential. All data quoted versus SCE. c) quasi-reversible Scan rate 200 mV/sec (p-p>100 mV). d) Data in reference 7 were adjusted to SCE from the internal ferricenium/ferrocene potential using a different, less accurate potential. These data assume Fc^+/Fc lies at +0.425 vs SCE. e) circumstantially acquired from cyclic voltammogram of $Ru(bpy)_2$(no)catH_2^+. Cyclic voltammogram taken in DCE.

Table II. Electronic Spectra of RuN_4L where N = bis-Bipyridine or tetra-Pyridine and L = (nn) or (no) or (oo) orthophenylenes.

Complex (solvent)	λ_{max}/cm^{-1}	log ε	f[a]	Assignment
bpy(nn)catH_4	21 100	3.73		Ru(II) -> π^*(1) bpy
(MeCN)	29 700	3.62		Ru(II) -> π^*(2) bpy
	34 200	4.4		π bpy -> π^*(1) bpy
	40 800	4.09		π bpy -> π^*(2) bpy
py(nn)catH_4	26 000	4.22		Ru(II) -> π^*(1) py
(10% Aq HOAc)				
bpy(no)catH_2	15 000sh			$3b_1$ (no)cat-> π^*(1)bpy
(DCE)	18 900	3.95		Ru(II) -> π^*(1) bpy
	23 650sh			d-d ?
	27 000	3.90		Ru(II) -> π^*(2) bpy
	33 750	4.73		π bpy -> π^*(1) bpy
bpy(oo)cat	13 700(br)	3.64		$3b_1$ (oo)cat->π^*(1) bpy
(DCE)	16 200	3.96		Ru(II) -> π^*(1) bpy
	20 850-24 650			$3b_1$ (oo)cat -> π^*(2) bpy
	26 300	4.03		Ru(II) -> π^*(2) bpy
	30 050	4.06		π (oo)cat -> π^* (oo)cat
py(oo)cat	19 200sh			$3b_1$ (oo)cat->π^*(1) py
(DCE)	21 700	4.15		Ru(II) -> π^*(1) py
	25 400	4.07		Ru(II) -> π^*(1) py, d-d ?
	29 400	3.91		$3b_1$ -> π^*(2) py
bpy(oo)catH	18 800	3.88		Ru -> π^*(1) bpy

(DCE)	27 400	3.95		Ru -> π^*(2) bpy
py(oo)catH	25 200	4.21		Ru -> π^*(1) py
(DCE)				
bpy(nn)sqH_2	16 000	4.05	0.11	Ru(II) -> $3b_1$ sqH_2
(MeCN)	18 700sh			Ru(II) -> π^*(1) bpy
	20 150	3.96	0.10	Ru(II) -> π^*(1) bpy
	22 000sh			$9a_1$ -> π^*(1) bpy LLCT, d-d
	23 000	3.88		$2a_2$ -> $3b_1$ intraligand (nn)sq
	28 650	3.91		Ru(II) -> π^*(2) bpy
py(nn)sqH_2	15 150	4.02	0.10	Ru(II) -> $3b_1$ (nn)sq
(DCE)	18 700			py(nn)q impurity
	25 450	4.16	0.46	Ru(II) -> π^*(1) py
bpy(no)sqH	14 700	4.00	0.13	Ru(II) -> $3b_1$[b]
(DCE)	19 100	3.95	0.13	Ru(II) -> π^*(1) bpy
	20 200sh	3.93		Ru(II) -> π^*(1) bpy
	26 200	3.99		$2a_2$ -> $3b_1$ intraligand (no)sq
	28 550	4.00		Ru(II) -> π^*(2) bpy
bpy(oo)sq	11 250	4.29	0.14	Ru(II) -> $3b_1$ sq
(DCE)	17 250sh			$3b_1$ (oo)sq-> π^*(1) bpy
	19 400sh			Ru(II) -> π^*(1) bpy
	20 300	3.87	0.12	Ru(II) -> π^*(1) bpy
	29 050	4.02		Ru(II) -> π^*(2) bpy +
				$2a_2$ -> $3b_1$ intraligand (oo)sq
py(oo)sq	10 600	3.95	0.11	Ru(II) -> $3b_1$ sq
(DCE)	18 000			$3b_1$ (oo)sq-> π^*(1) py
	27 900	4.12	0.40	Ru(II) -> π^*(1) py
	40 950	4.13		π py -> π^*(1) py

bpy(nn)qH_2	19	400	4.34	0.26	Ru(II) -> $3b_1$ qH_2
(MeCN)	22	450(sh)	3.89	0.09	Ru(II) -> π^*(1) bpy
	30	850(sh)			Ru(II) -> π^*(2) bpy
	35	600	4.61		π bpy -> π^*(1) bpy
	41	300	3.66		π bpy -> π^*(2) bpy
py(nn)qH_2	18	700	4.14	0.22	Ru(II) -> $3b_1$ qH_2
(DCE)	31	900	4.07	0.31	Ru(II) -> π^*(1) py
	34	600(sh)	4.03		π (nn)qH -> π^* qH
	41	800	4.44		π py -> π^*(1) py
bpy(no)qH	17	400	4.10	0.21	Ru(II) -> $3b_1$ qH
(DCE)	20	500	3.88		spin forbidden transition
	23	000			Ru(II) -> π^*(1) bpy
	27	350	3.93		Ru(II) -> π^*(2) bpy
bpy(oo)q	15	600	4.12	0.23	Ru(II) -> $3b_1$ q
(DCE)	22	500(sh)			$9a_1$ -> $3b_1$ intraligand q
	25	600	3.88		Ru(II) -> π^*(1) bpy
	27	800	3.88		$2a_2$ -> $3b_1$ intraligand q,b
py(oo)q	15	600	3.76	ca0.32	Ru(II) -> $3b_1$ q
(DCE)	30	000	4.06		Ru(II) -> π^*(1) py

---

a) Oscillator strength calculated using Eqn.4.2, p.162 of Ref.61. b label since the (no) ligand is not strictly C_2 in symmetry.

Table III Transition Bandwidths

Bipyridine complexes		Pyridine complexes	
Ru ---> sqH_2 (nn)	2100	Ru ---> sqH_2 (nn)	2050 cm^{-1}
Ru ---> sqH (no)	2200	Ru ---> sq (oo)	2400
Ru ---> sq (oo)	1400	Ru ---> qH_2 (nn)	3450
Ru ---> qH_2 (nn)	2500	Ru ---> q (oo)	5300
Ru ---> qH (no)	3800		
Ru ---> q (oo)	3950[a]		

a) Halfbandwidth data for Ru(II)(oo)q derivatives were in error (too small) by a factor of two in the previous report.[7]

Catecholoid $\underset{-nH^+ \; -e^-}{\overset{-nH^+ \; -e^-}{\rightleftharpoons}}$ Semiquinonoid $\underset{+e^-}{\overset{-e^-}{\rightleftharpoons}}$ Quinonoid

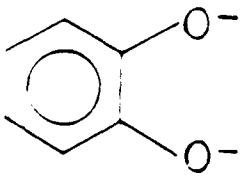

(oo)Cat

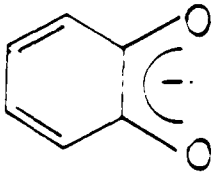

(oo)sq

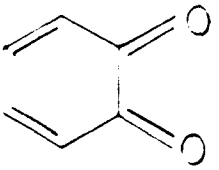

(oo)q

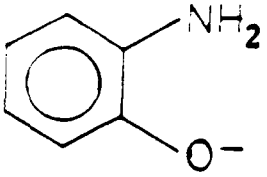

$(no)CatH_2$

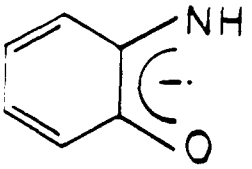

(no)sqH

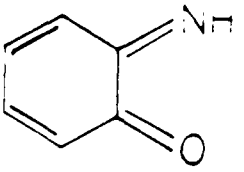

(no)qH

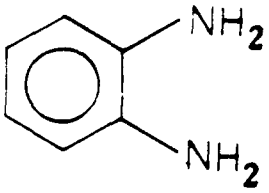

$(nn)CatH_4$

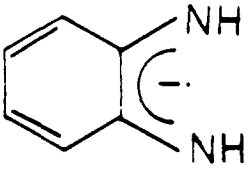

$(nn)sqH_2$

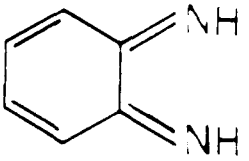

$(nn)qH_2$

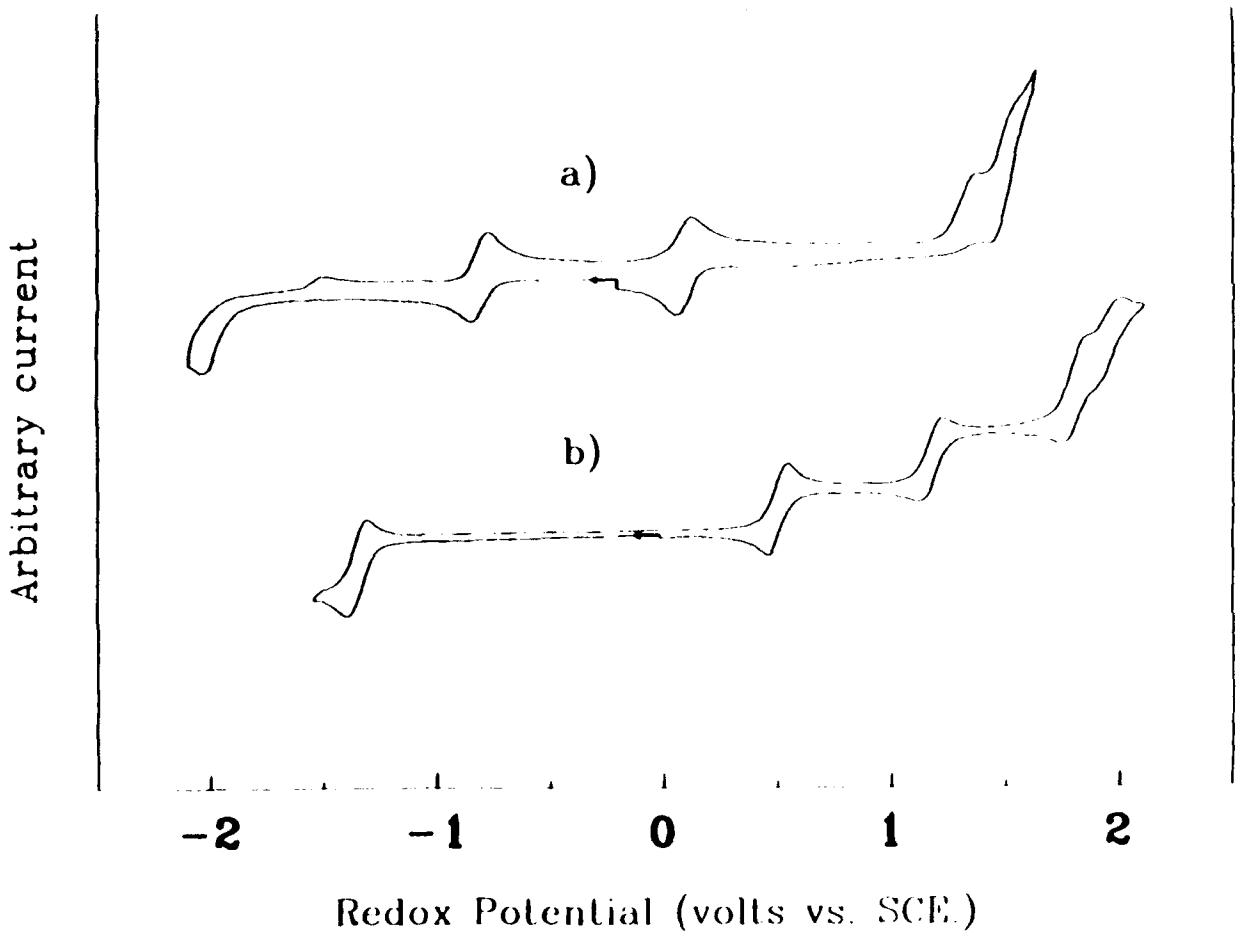
a)
b)
Arbitrary current
-2
-1
0
1
2
Redox Potential (volts vs. SCE)

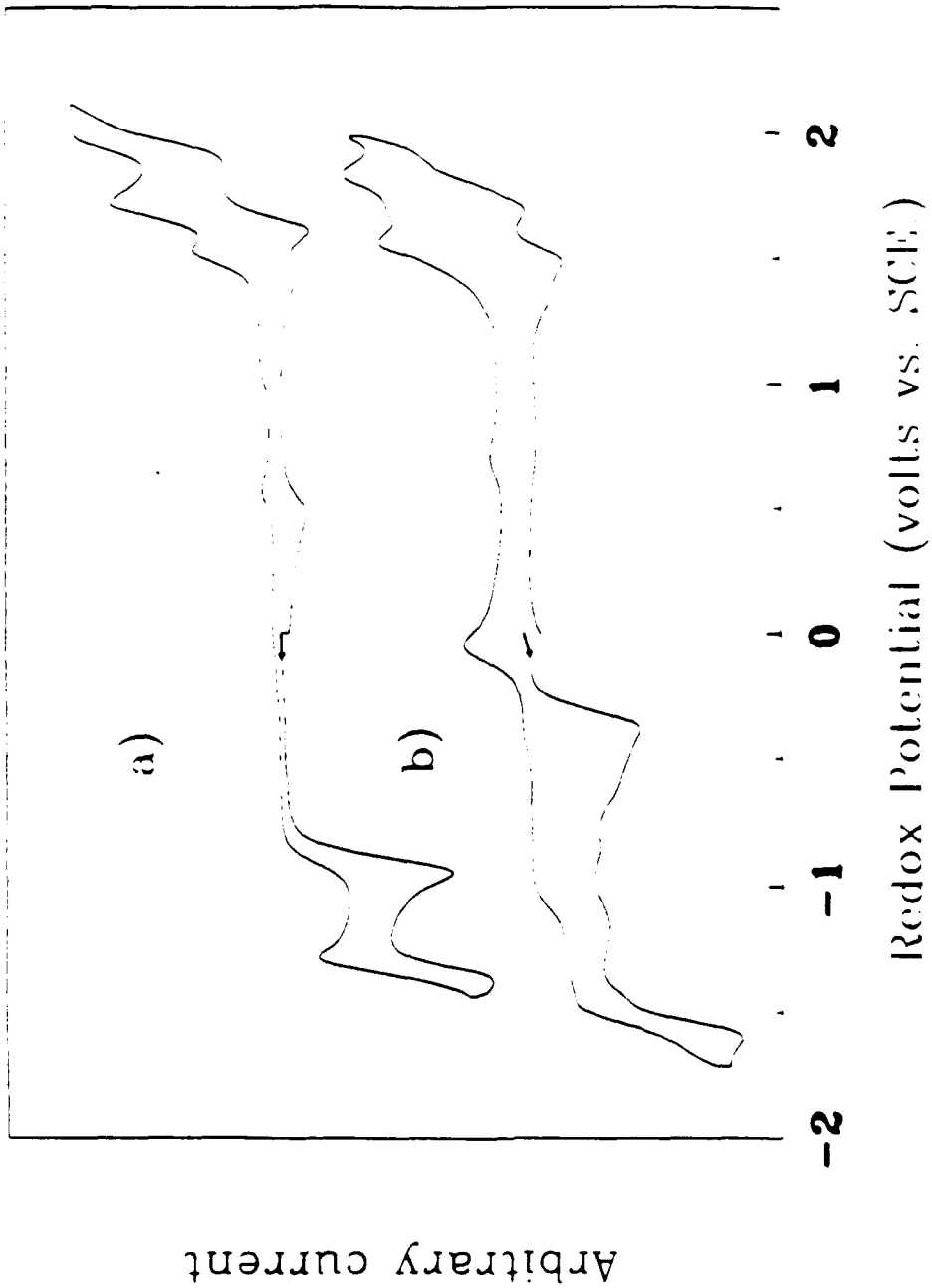
a)
b)
-2
-1
0
1
2
Redox Potential (volts vs. SCE)
Arbitrary current

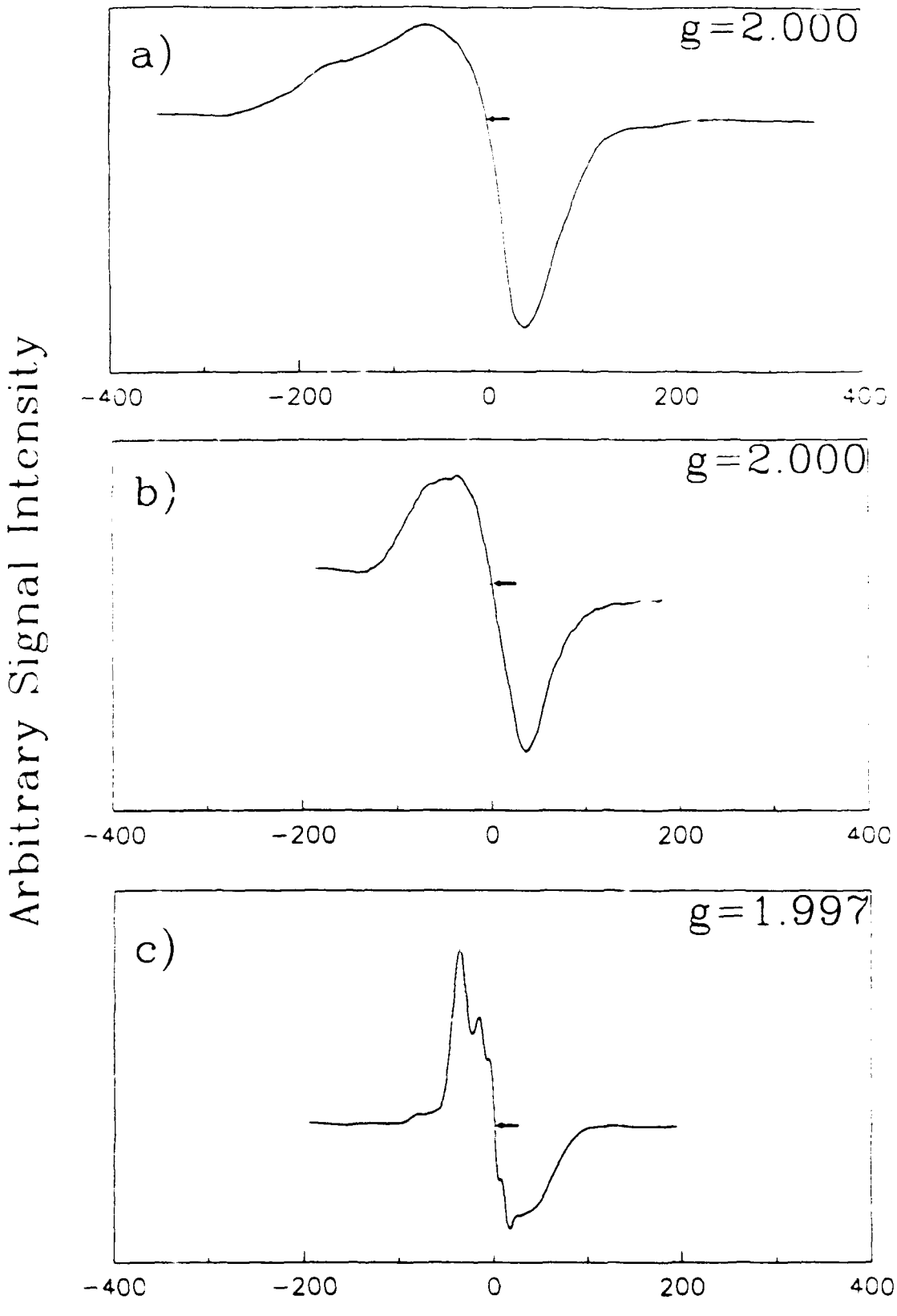
a)
g=2.000
-400
-200
0
200
400
b)
g=2.000
-400
-200
0
200
400
c)
g=1.997
-400
-200
0
200
400
Arbitrary Signal Intensity
Relative Magnetic Field Strength

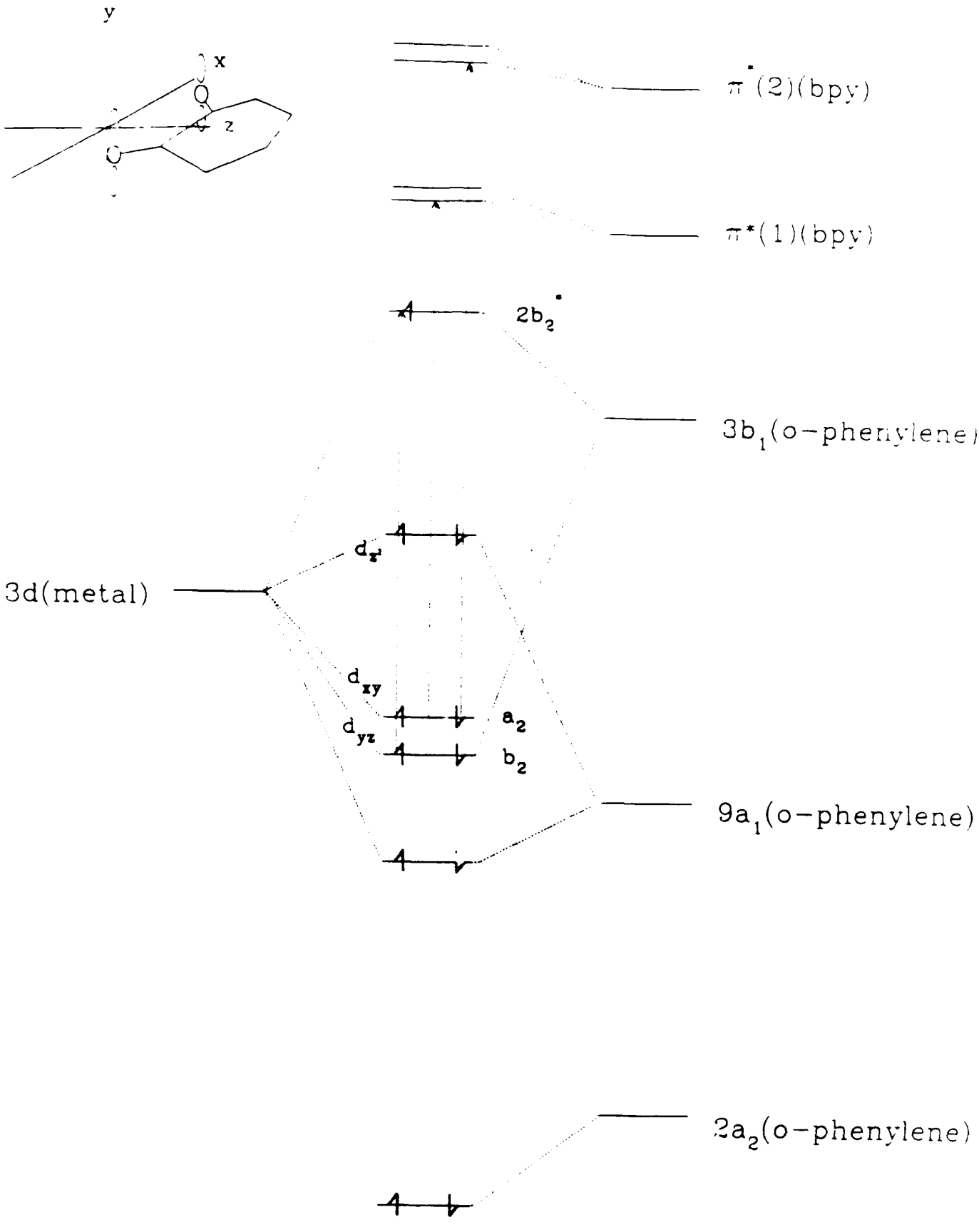
y
x
z
π*(2)(bpy)
π*(1)(bpy)
2b2
3b1(o-phenylene)
3d(metal)
dz²
dxy
dyz
a2
b2
9a1(o-phenylene)
2a2(o-phenylene)

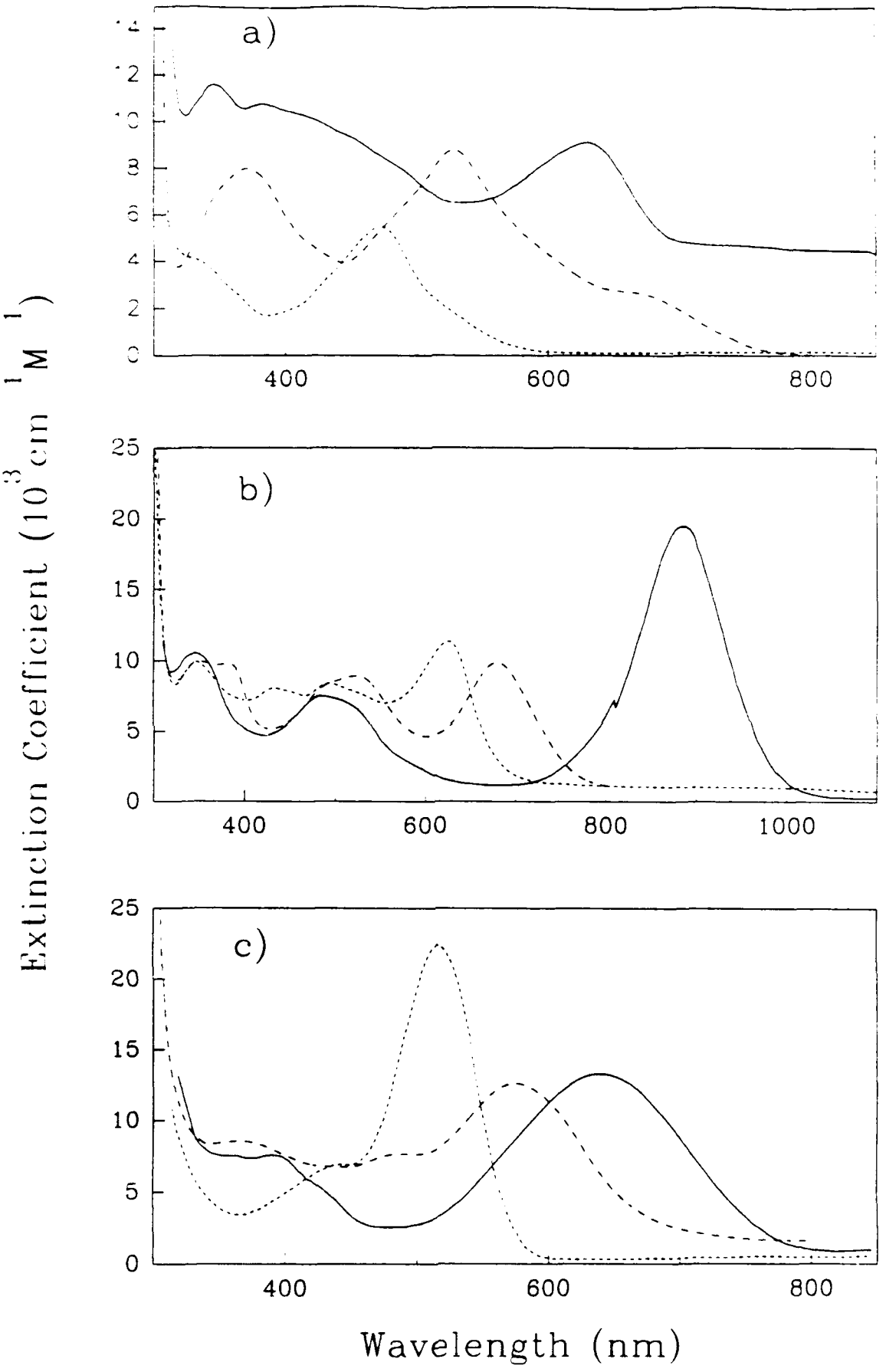
a)
b)
c)
Extinction Coefficient (10^3 cm^{-1} M^{-1})
Wavelength (nm)
400
600
800
1000
0
2
4
6
8
10
12
5
15
20
25

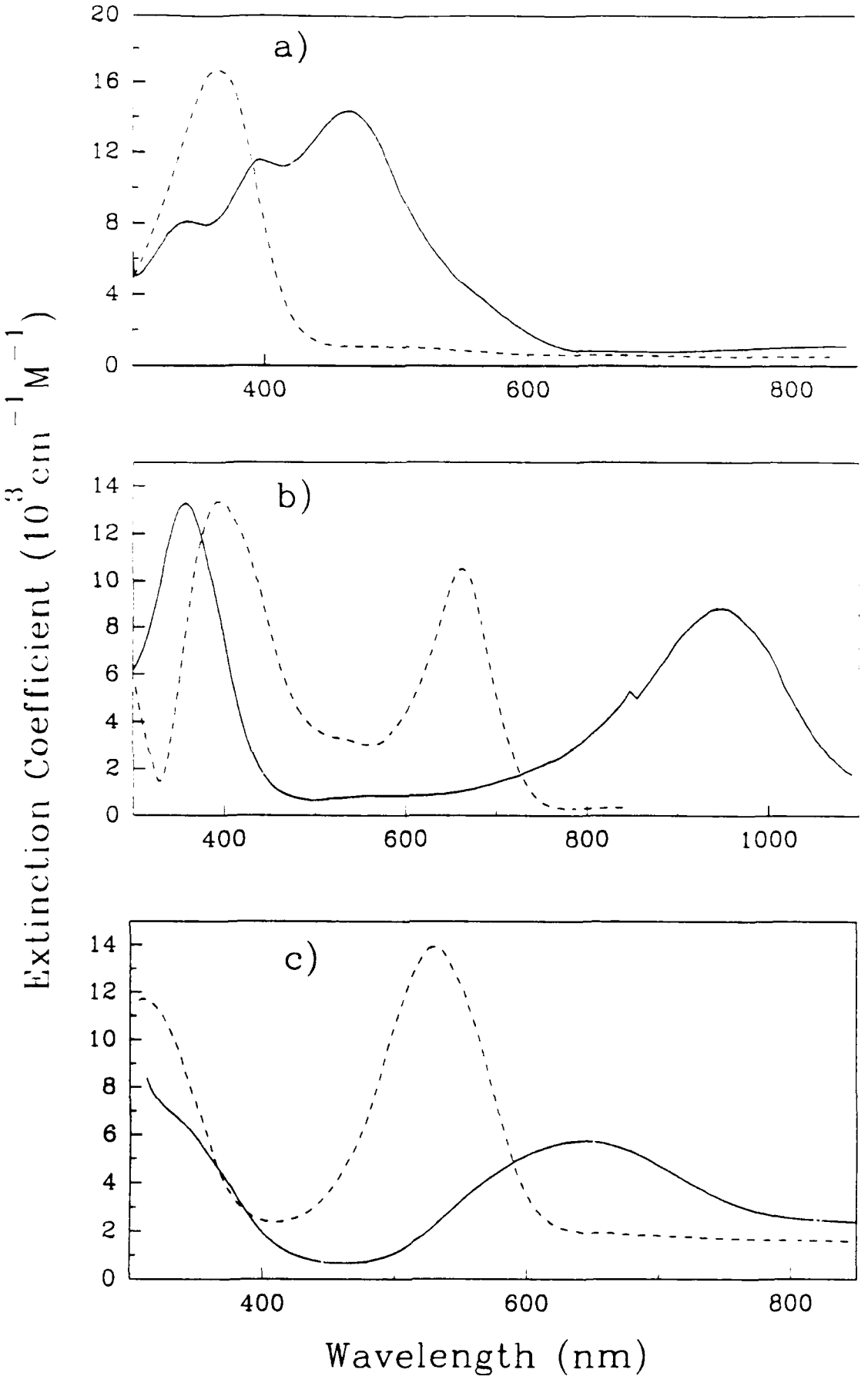
a)
b)
c)
Extinction Coefficient (10^3 cm^{-1} M^{-1})
Wavelength (nm)
0
4
8
12
16
20
400
600
800
2
6
10
14
1000

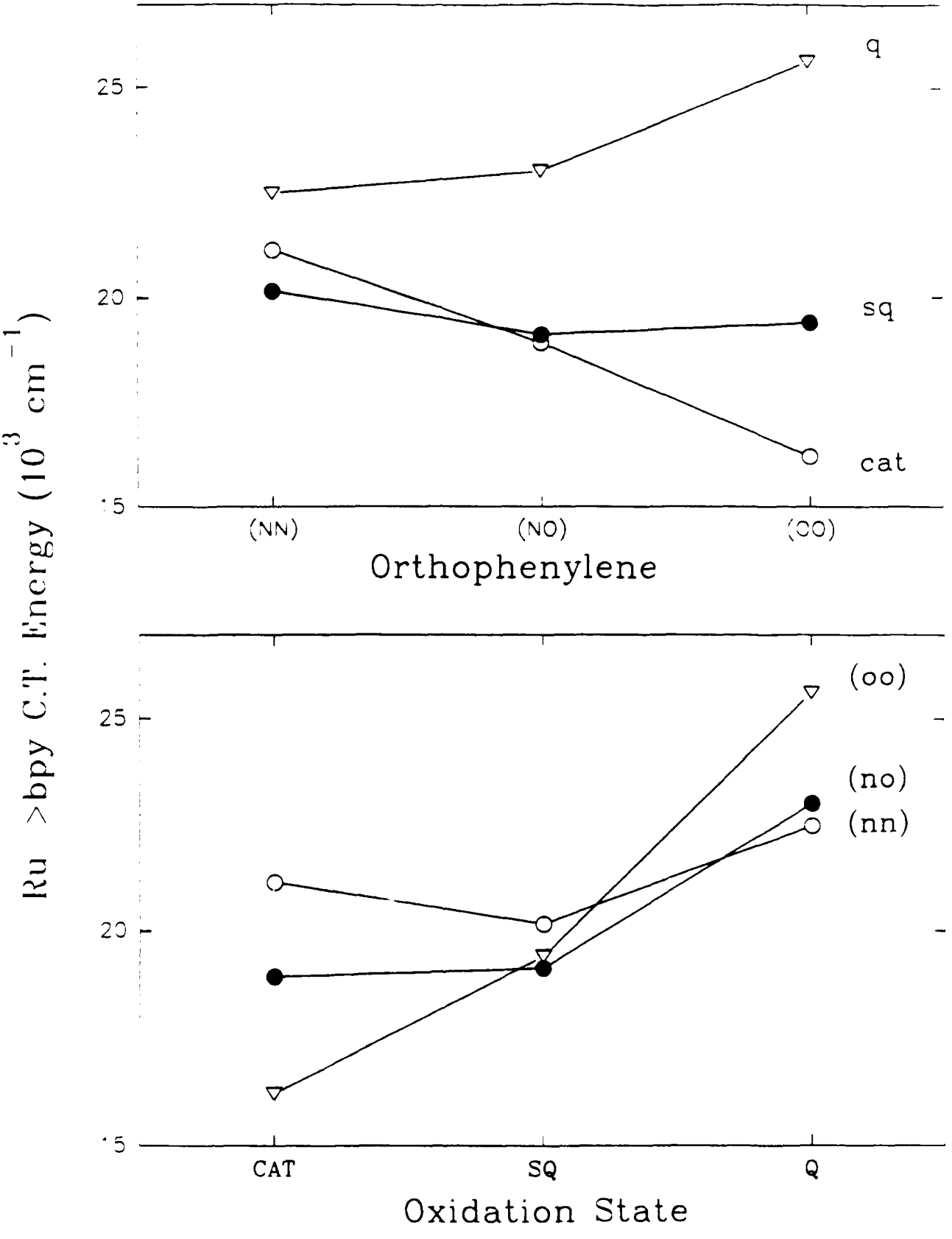
Ru >bpy C.T. Energy (10^{3} cm^{-1})
25
20
15
q
sq
cat
(NN)
(NO)
(OO)
Orthophenylene
25
20
15
(oo)
(no)
(nn)
CAT
SQ
Q
Oxidation State

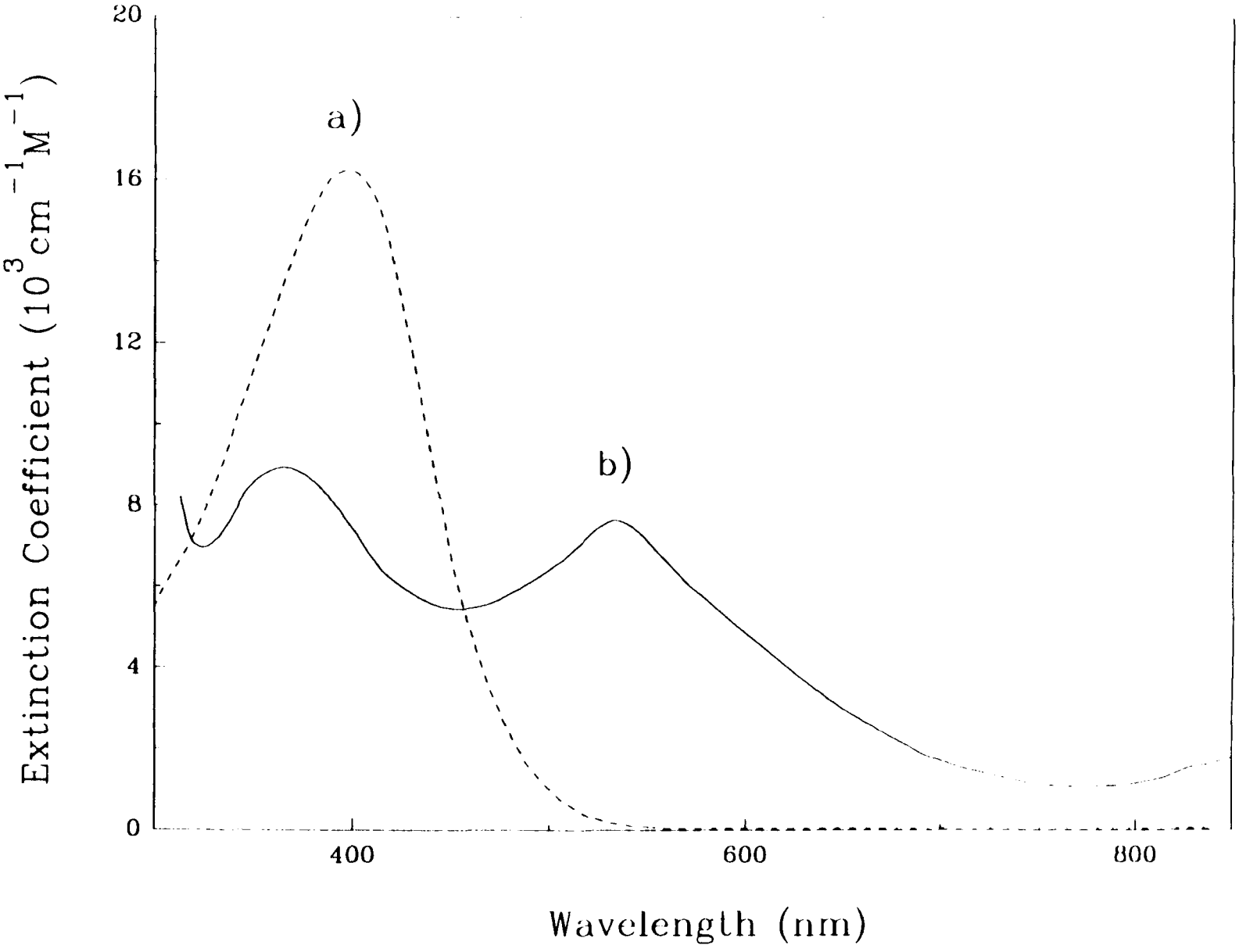
20
16
12
8
4
0
a)
b)
400
600
800
Extinction Coefficient ($10^3 cm^{-1} M^{-1}$)
Wavelength (nm)